UltraRapid Communication

Role of Asymmetric Dimethylarginine in Vascular Injury in Transgenic Mice Overexpressing Dimethylarginie Dimethylaminohydrolase 2

Kazuhiro Hasegawa, Shu Wakino, Satoru Tatematsu, Kyoko Yoshioka, Koichiro Homma, Naoki Sugano, Masumi Kimoto, Koichi Hayashi, Hiroshi Itoh

Abstract—Dimethylarginie dimethylaminohydrolase (DDAH) degrades asymmetric dimethylarginine (ADMA), an endogenous nitric oxide (NO) synthase inhibitor, and comprises 2 isoforms, DDAH1 and DDAH2. To investigate the in vivo role of DDAH2, we generated trangenic mice overexpressing DDAH2. The transgenic mice manifested reductions in plasma ADMA and elevations in cardiac NO levels but no changes in systemic blood pressure (SBP), compared with the wild-type mice. When infused into wild-type mice for 4 weeks, ADMA elevated SBP and caused marked medial thickening and perivascular fibrosis in coronary microvessels, which were accompanied by ACE protein upregulation and cardiac oxidative stress. The treatment with amlodipine reduced SBP but failed to ameliorate the ADMA-induced histological changes. In contrast, these changes were abolished in transgenic mice, with a reduction in plasma ADMA. In coronary artery endothelial cells, ADMA activated p38 MAP kinase and the ADMA-induced ACE upregulation was suppressed by p38 MAP kinase inhibition by SB203580. In wild-type mice, long-term treatment with angiotensin II increased plasma ADMA and cardiac oxidative stress and caused similar vascular injury. In transgenic mice, these changes were attenuated. The present study suggests that DDAH2/ADMA regulates cardiac NO levels but has modest effect on SBP in normal conditions. Under the circumstances where plasma ADMA are elevated, including angiotensin II–activated conditions, ADMA serves to contribute to the development of vascular injury and increased cardiac oxidative stress, and the overexpression of DDAH2 attenuates these abnormalities. Collectively, the DDAH2/ADMA pathway can be a novel therapeutic target for vasculopathy in the ADMA or angiotensin II–induced pathophysiological conditions. (***Circ Res*. 2007;101:e2-e10.**)

Key Words: DDAH2 ■ ADMA ■ angiotensin II

Asymmetric dimethylarginine (ADMA) is an endogenous competitive inhibitor of nitric oxide synthase (NOS). Substantial evidence has been accumulated that plasma ADMA mediates the endothelial dysfunction and serves as a marker of risk for cardiovascular disease.[1–3] ADMA is degraded by the enzyme, dimethylarginine dimethylaminohydrolase (DDAH), and would subsequently affect NO metabolism. It has been demonstrated that DDAH is composed of 2 isoforms, DDAH1 and DDAH2,[4] each of which stems from different chromosomes and differs in several aspects. DDAH1 and 2 appear to have distinct tissue distributions, with DDAH1 predominating in the tissues that express nNOS and DDAH2 being coexpressed with eNOS in highly vascularized tissues.[5] Moreover, in cultured human endothelial cells, DDAH1 is uniformly distributed in the cytosol and nucleus, whereas DDAH2 is found only in the cytosol.[6] The different characteristics between these 2 isoforms suggest different physiological functions.

Physiological function of DDAH1 has been elucidated by the studies using transgenic (TG) mice overexpressing DDAH1[7] and DDAH1 knockout (KO) mice.[8] In TG mice, tissue DDAH1 expression is increased and the plasma ADMA level is markedly reduced.[7] The reduction in ADMA levels is associated with a doubling of urinary excretion of nitric oxide metabolites and results in decreases in systemic vascular resistance and blood pressure. DDAH1 TG mice also exhibits enhanced ability for angioadaptation in response to an ischemic stimulus.[9] Furthermore, in cardiac transplantation, DDAH1 TG mice show suppressed immune responses probably because of increased myocardial NO generation and to reduced superoxide anion production.[10] In DDAH1 KO mice, plasma ADMA is increased and NO production is reduced, which increases systemic vascular resistance and elevates systemic blood pressure.[8] In contrast to DDAH1, in vivo function of DDAH2 has not been fully elucidated. It has been reported that DDAH1 protein expression remains un-

Original received December 23, 2006; resubmission received May 30, 2007; revised resubmission received June 18, 2007; accepted June 18, 2007.
From the Department of Internal Medicine (K.H., S.W., S.T., K.Y., K.H., N.S., K.H., H.I.), Keio University, Tokyo, and the Department of Nutritional Science (M.K.), Okayama Prefectural University, Okayama, Japan.
Correspondence to Shu Wakino, MD, Department of Internal Medicine, Keio University, 35 Shinanomachi, Shinjuku-ku, Tokyo, Japan, 160-8582. E-mail swakino@sc.itc.keio.ac.jp

Circulation Research is available at http://circres.ahajournals.org DOI: 10.1161/CIRCRESAHA.107.156901

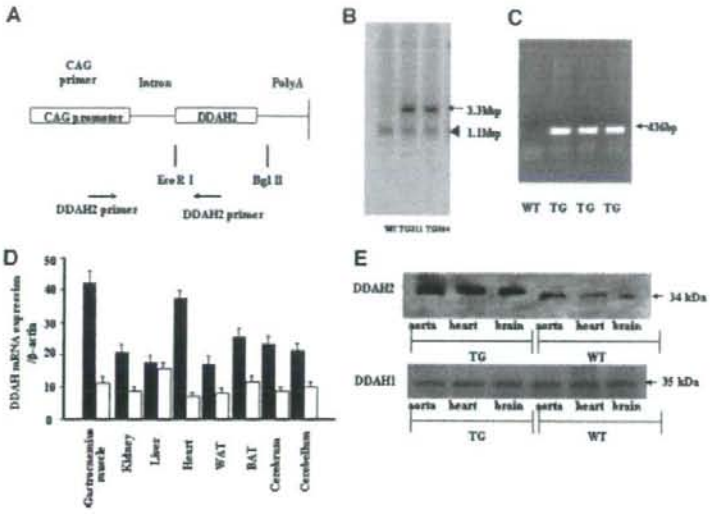

Figure 1. Genotyping of DDAH2 transgenic (TG) mice and their transgene expression. A, The construct used for the foundation of DDAH2 transgenic mice contains a 3.3-kb fragment from the CAG promoter, a 1-kb murine DDAH2 cDNA fragment, an intron, and β-globin polyadenylation sequences. Restriction sites and primers used in the PCR are indicated. B, Southern blotting in which an arrow indicates bands (3.3 kb) corresponding to transgene-derived DDAH2. An arrowhead indicates endogenous mouse DDAH2 gene (1.1kb). C, A representative PCR analysis shows that 436bp-PCR products contain sequences of the DDAH2 transgene. D, Quantitative RT-PCR analysis of DDAH2 expression in various tissues from TG mice (filled bars) and WT littermates (open bars). E, Immunoblot analysis reveals that TG mice manifest increased DDAH2, but not DDAH1, protein expression.

changed under many conditions in which vascular DDAH activity declines.[11,12] It is speculated therefore that DDAH2 rather than DDAH1 plays a pivotal role in modulating ADMA metabolism in vascular tissues.

Recently, there has been reported substantial interaction between ADMA and renin-angiotensin system (RAS), an pivotal mechanism mediating the development of vascular injury. Antihypertensive agents, including angiotensin converting enzyme (ACE) inhibitors and angiotensin type 1 receptor blockers (ARB), have been shown to decrease plasma ADMA in a couple of studies.[13,14] Furthermore, Suda et al[15] demonstrated that chronic treatment with ADMA caused vascular lesions and superoxide production in both wild-type (WT) and eNOS-deficient mice, and these changes were prevented by either ACE inhibitor or ARB treatment. These studies suggest an intimate link between ADMA and renin-angiotensin system (RAS) that does not necessarily depend on NO. It is conjectured therefore that the alteration in ADMA metabolism by DDAH would offer favorable action in the development of vascular injury induced by angiotensin II (Ang II).

To delineate the role of ADMA and Ang II–induced changes of the ADMA-DDAH system in vascular injury, we attempted to generate TG mice overexpressing DDAH2. These mice exhibited decreased plasma ADMA levels as compared with those in the WT littermate, whereas blood pressure did not differ between these WT and TG mice. Furthermore, overexpression of DDAH2 attenuated the vascular lesion induced by continuous administration of ADMA or Ang II. Finally, chronic ADMA elevation upregulated the ACE protein expression in the vascular tissue, which was downregulated in DDAH2 TG mice. In vitro studies demonstrated that p38 mitogen-activated protein (MAP) kinase mediated the upregulation of ACE by ADMA. The present results indicate a novel functional link between the DDAH/ADMA system and the RAS in the vascular tissue and implicates vascular DDAH2 as a counter-regulatory mechanism against tissue RAS.

Materials and Methods

Generation of DDAH2 Transgenic Mice

Murine DDAH2 cDNA containing its full-length open-reading frame (ORF) was cloned as described previously.[16] The cDNA was inserted downstream of the ubiquitous strong CAG promoter of the pCAGGS vector (Figure 1A).[17] For the production of transgenic mice, the SalI-HindIII fragment of pCAGGS-DDAH2 was microinjected into 1-cell fertilized mouse embryos obtained from superovulated C57BL/6 X C3H mice as previously described.[18] Founder mice were identified by Southern blot analysis of EcoRI/BglII-digested tail genomic DNA with the DDAH2 ORF as a probe. The positive transgenic founders were then crossed with wild-type C57BL/6 mice (Charles River Japan Inc, Yokohama, Japan) to obtain the F1 generation. Genomic DNA was isolated from tail biopsies at 3 weeks of age using a DNeasy kit (Qiagen Inc) and subjected to Southern blot analysis to identify the transgene. Southern blots were interrogated with a ^{32}P-labeled probe to the EcoRI and BglII fragment of murine DDAH II cDNA. Genomic DNA digested by EcoRI and BglII yielded a single band of the expected size in TG mice only (Figure 1B). Additional screening of genomic DNA samples was done by polymerase chain reaction using transgene-specific oligonucleotide primers GATGCAGCTAGTGACTGTCTCTTT (CAG promoter side) and AGAGGGAAAAAGATCT CAGTGGTAT (DDAH2 gene side) (Figure 1A), which amplify a 436-bp region spanning the junction between the CAG promoter and the DDAH2 gene (Figure 1C). Increased protein expressions of DDAH2 were confirmed by immunoblotting using antibody against DDAH2 (Abcam; Figure 1E).

Experimental Protocol

Eight-week-old heterozygous male TG mice and their age-matched wild-type male littermates were used in these experiments. To examine the effect of DDAH2 overexpression on ADMA-induced vascular lesions, the following groups were studied: WT and TG mice that received subcutaneous saline infusion, or subcutaneous ADMA infusion (60 mg/kg/d, Sigma), or WT mice that received subcutaneous ADMA (60 mg/kg/d) infusion plus amlodipine (10 mg/kg, Wako Pure Chemical Industries Ltd) in drinking water. Saline or ADMA was infused via an implanted osmotic minipump for 4 weeks (Model 2004; Alzet). The effect of DDAH2 overexpres-

sion on Ang II–induced vascular lesions was also examined by assigning the mice into the following groups: WT and TG mice that received subcutaneous saline infusion, or subcutaneous Ang II infusion (1 μg/kg/min), or WT and TG mice that received subcutaneous Ang II infusion plus amlodipine (10 mg/kg) in drinking water. In all of these groups, the treatments were performed for 2 weeks. Systolic blood pressure (SBP) was measured by tail-cuff plethysmography (Visitech 2000, Visitech Systems) on 3 consecutive days and values were averaged. These studies were performed in accordance with the animal experimentation guideline of Keio University School of Medicine.

Histological Analysis

The mice were euthanized by inhalation of overdose diethyl ether (Wako Pure Chemical Industries Ltd). The aorta was cannulated and perfused with 4% paraformaldehyde solution under physiological pressure. Then, the heart was removed and embedded in paraffin, and the tissue slices were stained with Masson-trichrome solutions. The sections were scanned using a light microscope equipped with a 2-dimensional analysis system (IBAS; Carl Zeiss). The extent of medial thickening and perivascular fibrosis of the coronary arteries was evaluated by the ratio of medial thickness to internal diameter and the ratio of perivascular fibrosis area to total vascular area, respectively. In each heart, more than 10 coronary microvessels (internal diameter, 30±4 μm) were evaluated, and the average value was adopted for the pathological index in each heart. Histological findings were obtained in a blinded fashion by 3 independent researchers.

Biolochemical Measurements

Plasma and tissue concentrations of L-arginine, ADMA, and symmetric dimethylarginine (SDMA) were measured by HPLC.[19] DDAH enzyme activity was assayed as described previously.[12] The NO concentration of tissue extracts were determined using Quantichrom Nitric Oxide Assay Kit (Bioassay Systems). To detect in situ generation of ROS, fluorescece micrography with dihydroethidium was performed as previously described.[20]

Immunoblotting

Immunoblotting was performed as described previously,[21] using specific antibodies against DDAH1 (Abcam), DDAH2 (Abcam), mouse ACE (Chemicon), human ACE (Santa Cruz Biotechnology), p38MAPK, phospho-specific p38MAPK (Thr^{180}/Thr^{182}) (both from New England Biolabs), or β-actin (Sigma). Tissue samples from each animal or cell lysates were obtained by homogenizing tissue or cultured cells in lysis buffer as described previously.[22,23] For quantification of ACE protein, membrane fraction from the cardiac tissue was isolated as described previously.[23]

Quantitative RT-PCR

Total RNA was isolated from various tissues from TG and WT littermate mice. Preparation of DNase-treated total RNA, reverse transcription, and PCR protocols were performed. We monitored the levels of PCR products with an ABI PRISM 7700 sequence detection system and analyzed them with ABI PRISM 7700 SDS software (Applied Biosystems Japan Ltd). The relative abundance of transcripts was normalized to constitutive expression of β-actin (Figure 1D).

Cell Culture

Human coronary artery endothelial cells (HCAECs; Clonetics) grown to confluence in 6-cm dishes were rendered quiescent for 24 hours before stimulation with 10μmol/L ADMA or 100 nmol/L AngII (both from Sigma). To block the p38 or p44/42 (ERK) MAP kinase, cells were treated with SB203580 or PD98059 (both from Calbiochem) for 60 minutes before stimulation, respectively.

Statistics

Data were expressed as the mean±SEM. Data were analyzed using 1-way or 2-way analysis of variance, as appropriate, followed by a Bonferroni's multiple comparison post hoc test. Probability values less than 0.05 were considered statistically significant.

Results

Generation of DDAH2 TG Mice

TG mice did not differ from the WT littermates in general appearance; they manifested normal development and were fertile. TG mice offsprings were obtained in a Mendelian ratio. Detailed necropsies revealed no anatomical abnormalities. We obtained 2 lines of TG mice, line 204 and line 211, as shown in Figure 1B. According to the results of Southern blotting, quantitative analysis demonstrated that 4 copies of the transgene were integrated in TG 204 transgenic mice and 6 copies in TG 211 mice, respectively. However, the expression levels of DDAH2 in the vasculature were not different between the 2 lines and both lines developed normally and appeared the same phenotype. These 2 lines were propagated and were used for subsequent experiments. The representative data shown below were obtained from the line 211 mice. 436bp-PCR products containing sequences of the DDAH2 transgene in combination with the CAG promoter were detected in TG mice but not in WT mice (Figure 1C). As shown in Figure 1D, quantitative RT-PCR analyses revealed that DDAH2 was expressed in various tissues from TG mice (filled bars) and WT littermates (open bars). The CAG promoter has been reported to be strongly active in a variety of tissues. In our TG mice, the promoter drove higher expressions in the brown adipose tissue, the heart, and the skeletal muscle. Immunoblot analysis revealed that DDAH2 protein expression was increased in TG mice, compared with that in WT littermates (Figure 1E). We further examined whether DDAH2 overexpression affected the expression levels of another isoform DDAH1, and found that DDAH1 protein expressions were unaltered in TG mice (Figure 1E).

Phenotypic Analysis of DDAH2 TG Mice

At the age of 8 weeks, DDAH activities in skeletal muscle were significantly increased in TG mice (Figure 2A). Histological examinations of cross-sections of vascular tissues revealed that the CAG-driven DDAH2 was located in large part in vascular smooth muscle cells (SMCs), which were most prominently distributed just below the internal elastic lamina (Figure 2B). The endothelial layer indicated with arrowheads was less commonly transduced than SMCs. Plasma ADMA levels were reduced in TG mice (Figure 2C), whereas plasma SDMA and arginine levels were unaltered (data not shown). Local NOx levels in cardiac tissues were increased in TG mice as compared with those in WT mice (Figure 2D). SBP was unaltered in TG mice (Figure 2E).

Effects of DDAH2 Overexpression on the Degradation of Plasma ADMA

In WT mice, long-term treatment with ADMA (60 mg/kg/d) increased plasma ADMA concentrations (2.87±0.33 μmol/L, n=5), a level comparable to that observed in pathophysiological conditions (2 to 10 μmol/L).[14] The elevation of the

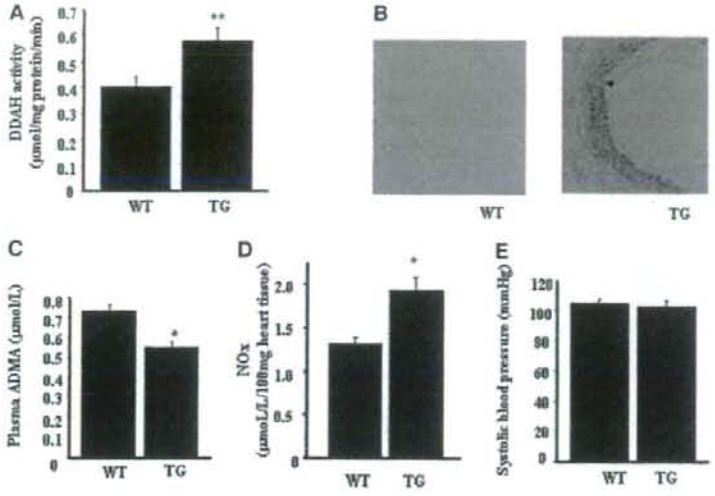

Figure 2. Baseline characteristics of DDAH2 TG mice. A, DDHA activity measured in skeletal muscle. B, Histological examinations of cross-sections reveal that the components in blood vessels transduced by CAG-driven DDAH2 are mostly vascular smooth muscle cells. C, Plasma ADMA levels of both WT and TG mice. D, Local NOx levels in heart homogenates from WT and TG mice. E, Systolic blood pressure of TG and WT mice. *$P<0.05$ vs WT mice, n=5. **$P<0.01$ vs WT mice, n=5.

ADMA level, however, was prevented in DDAH2 TG mice (0.95±0.05 μmol/L, n=5, Figure 3A). Similarly, the treatment with ADMA elevated SBP in WT mice (125±4 mm Hg, n=5), but had no effect in TG mice (105±5 mm Hg, n=5, Figure 3B). In TG mice, the administration of ADMA reduced the NOx level in cardiac tissue. Although ADMA also reduced the cardiac NOx levels in TG mice, the level achieved remained within the range observed in WT mice (ie, saline in WT, Figure 3C).

Effects of DDAH2 Overexpression on ADMA-Induced Vascular Lesions

Long-term treatment with ADMA caused marked medial thickening and perivascular fibrosis in coronary microvessels of WT mice. The vascular tissue damages by ADMA were totally attenuated in TG mice (Figure 4A to 4C). To eliminate the possibility that reduced blood pressure contributed to these morphological changes in TG mice, we treated the ADMA-infused WT mice with amlodipine. Amlodipine treatment failed to mitigate the histological deterioration by ADMA, although the blood pressure was reduced to the same level as that observed in ADMA-infused TG mice (TG mice versus amlodipine-treated mice; 104±5 versus 105±5 mm Hg, n=5).

Effects of DDAH2 Overexpression on ADMA-Induced ROS Production and ACE Protein

We investigated the mechanism for the effects of DDAH2 overexpression on ADMA-induced vascular injury. Without ADMA administration (ie, saline), dihydroethidium staining revealed no difference in fluorescent signals between WT

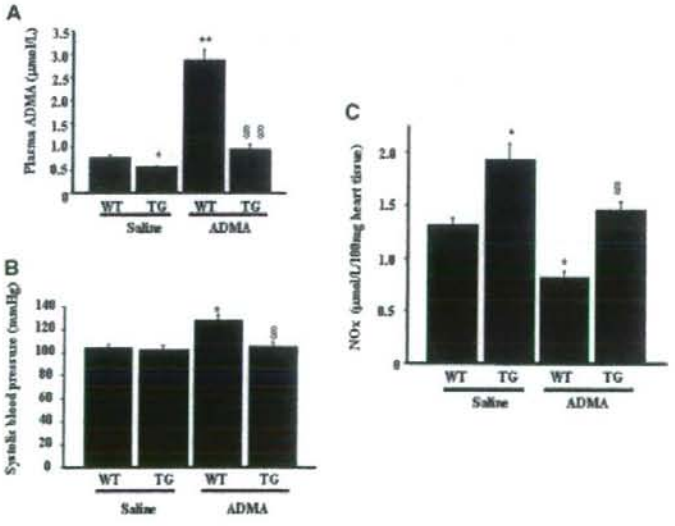

Figure 3. Effects of ADMA infusion on plasma ADMA levels, blood pressure, and cardiac NOx levels. A, Long-term treatment with ADMA caused an increase in plasma ADMA levels in WT mice, but not in TG mice. B, ADMA infusion elevated systolic blood pressure in WT mice, but had no effect in TG mice. C, ADMA infusion reduced NOx levels in cardiac tissues from WT mice, whereas the NOx levels in TG mice were maintained within the range of WT mice. *$P<0.05$ vs saline-infused WT mice, n=5. **$P<0.01$ vs saline-infused WT mice, n=5. §$P<0.05$ vs ADMA-infused WT mice, n=5. §§$P<0.01$ vs ADMA-infused WT mice, n=5.

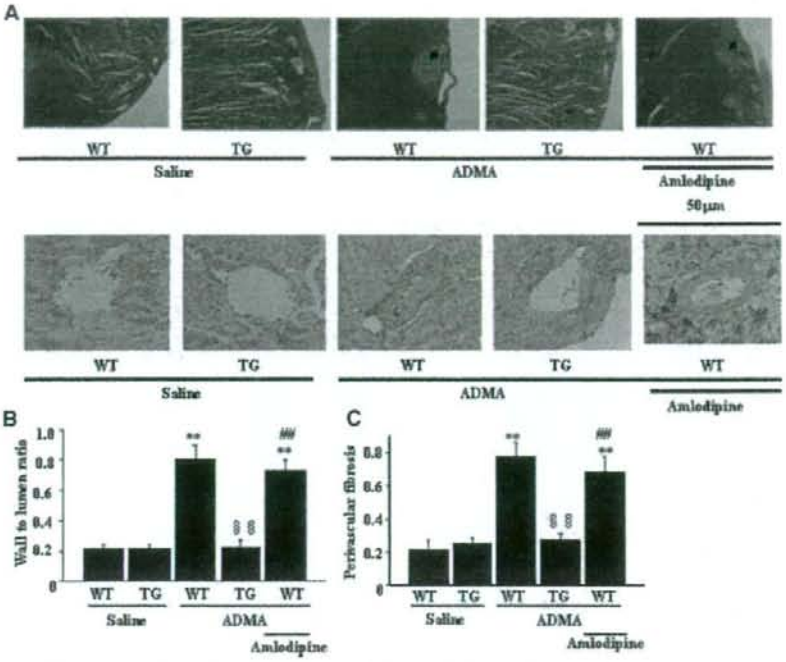

Figure 4. Effects of ADMA infusion on vascular lesions. A, Masson-trichrome staining showed that ADMA infusion caused marked vascular injury in WT mice, which was prevented in TG mice. Upper panels manifest low power micrographs of the left ventricle, whereas lower ones represent high power graphs. Amlodipine failed to ameliorate the ADMA-induced lesion. Quantification of coronary vascular lesion formation was assessed by wall to lumen ratio (B) and perivascular fibrosis (C). $^{**}P<0.01$ vs WT mice with saline infusion, n=5. §§$P<0.01$ vs WT mice with ADMA infusion, n=5. ##$P<0.01$ vs TG mice with ADMA infusion.

mice and TG mice (Figure 5A). When treated with ADMA, WT mice increased the cardiac fluorescent signals of dihydroethidium, whereas the enhanced signals were not observed in DDAH2 TG mice. Amlodipine did not suppress the ROS production induced by ADMA.

A recent study has demonstrated that the upregulation of ACE protein in ADMA-treated mice in vascular tissues.[15] The expression of the ACE protein in the heart was significantly upregulated in WT with the ADMA infusion, which was totally abolished in TG mice. (Figure 5B).

Effects of DDAH2 Overexpression on Ang II–Induced Vascular Lesions

The role DDAH2/ADMA in mediating the Ang II–induced vascular injury was examined. Two-week Ang II infusion caused similar magnitude of the elevation in systemic blood pressure in WT (143±6 versus 104±3 mm Hg, n=5) and TG mice (142±6 versus 102±4 mm Hg, n=5). Histological examination revealed that the Ang II infusion induced marked medial thickening and elicited prominent perivascular fibrosis in coronary microvessels of WT mice (Figure 6). These effects of Ang II, however, were attenuated in TG mice.

In WT mice, the treatment with Ang II elicited a substantial increase in plasma ADMA levels (from 0.72±0.04 to 1.48±0.15 μmol/L, n=5), and this effect was markedly prevented in TG mice (from 0.52±0.03 to 0.80±0.04 μmol/L, n=5, Figure 7A). In dihydroethidium staining, the cardiac fluorescent signals under basal conditions were not different between WT mice and TG mice (Figure 7B). When treated with Ang II, the fluorescent signals were increased in WT mice, but were markedly attenuated in TG mice. The continuous infusion of Ang II, however, failed to alter the ACE protein expression in either WT and DDAH2 TG mice (Figure 7C).

Role of p38 MAP Kinase in ADMA-Induced ACE Expression

We examined the molecular mechanism for the DDAH2/ADMA-mediated ACE expression in vitro, using HCAECs. ADMA (10 μmol/L) directly upregulated the ACE protein expression in HCAECs (Figure 8A). This effect was nearly completely prevented by the DDAH2 overexpression. Furthermore, ADMA enhanced the p38 MAP kinase activity, and this activation was abolished by SB203580, a p38 MAP kinase specific inhibitor, but not by PD98059, a specific p44/42 MAP kinase inhibitor (Figure 8B). Finally, SB203580, but not PD98059, prevented the ADMA-induced ACE upregulation in HCAECs (Figure 8C). In contrast, Ang II (100 nmol/L) had no effect on the ACE expression in HCAECs (Figure 8D).

Discussion

In the present study, we have generated TG mice overexpressing DDAH2 and have demonstrated that they mani-

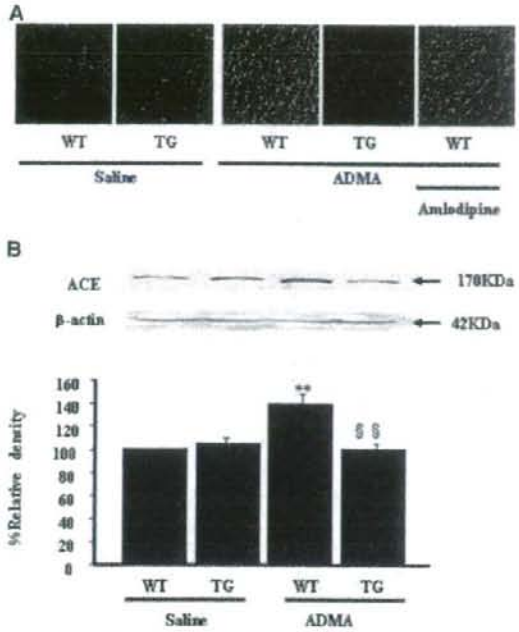

Figure 5. Effects of ADMA infusion on oxidative stress levels and ACE expression. A, Dihydroethidium staining revealed enhanced fluorescent signals in cardiac tissues from WT mice with ADMA. In TG mice, however, the treatment with ADMA did not augment the signals. Amlodipine had no effect on the ADMA-induced enhance signals. B, Immunoblotting showed that ADMA infusion increased ACE protein expression in heart homogenates from WT mice, but not in those from TG mice. $^{**}P<0.01$ vs WT mice with saline infusion, n=5. §§$P<0.01$ vs WT mice with ADMA infusion, n=5.

fest reduced plasma ADMA levels, although systemic blood pressure in TG mice does not differ from that in WT mice (Figure 2). When administered exogenously in WT mice, ADMA causes increases in systemic blood pressure (Figure 3) and induces prominent vascular injury (Figure 4). These alterations are totally abolished in TG mice overexpressing DDAH2. Furthermore, the fact that lowering blood pressure by amlodipine fails to prevent histological changes in TG mice implicates ADMA per se as a crucial factor mediating the vascular injury. It has been reported that plasma ADMA levels are elevated in several disorders, including chronic kidney disease,[3] atherosclerosis,[24] and diabetes,[25] in which disorders increased incidence of cardiovascular events ensue. The present demonstration therefore would lend support to the contention that ADMA contributes importantly to the development of vascular injury in various cardiovascular disease and the intervention to DDAH2 expression can provide therapeutic strategies for these diseases.

Of note, in contrast to DDAH1 TG mice,[7] the present study fails to show a reduction in blood pressure in DDAH2 TG mice (Figure 2E). The difference between these 2 models may bear on the plasma ADMA levels in these 2 TG mice. In DDAH1 TG mice, the reduction in plasma ADMA levels was approximately 60%,[7] whereas DDAH2 TG mice manifested 26% reductions under basal conditions (Figure 2). Nevertheless, the exogenous ADMA increased the blood pressure, reduced tissue NOx levels (Figure 3), and increased the vascular lesion in WT mice (Figure 4), and these changes were abolished in DDAH2 TG mice. These observations suggest that alterations in tissue DDAH2/ADMA and the subsequent NO accumulation play an important role in protecting tissue injury. In this regard, Leiper et al[4] demonstrate that DDAH1 has an expression pattern similar to that of neuronal NOS, whereas DDAH2 is distributed in the areas nearly parallel with eNOS. Alternatively, Suda et al[15] demonstrated that the 4-week ADMA infusion elicited coronary microvascular lesions, similar in magnitude in WT and eNOS-deficient mice, and the effects of ADMA could not be prevented by supplementation of L-arginine. Schulze et al[24] have also reported that pathophysiological concentrations of ADMA can regulate several gene expressions in human endothelial cells by the mechanisms that appear to be NO-independent. Collectively, the tissue injury induced by ADMA may not depend totally on the suppression of NO activity.

In the present study, we have demonstrated that the long-term ADMA administration causes prominent coronary microvascular lesions (Figure 4). Furthermore, these pathological changes are accompanied by the enhanced ROS generation and upregulation of ACE protein (Figure 5). In contrast, these changes are totally abolished in mice overexpressing DDAH2. It has been reported that ADMA increases cardiac lucigenin chemiluminescence,[15] and enhances intracellular O_2^- production via "uncoupling of NOS activity" in endothelial cells.[26] By inhibiting NOS activity, ADMA alters the balance between NO and superoxide production, leading to an increase in oxidative stress within the vessel and myocardium.[27] Finally, it has also been demonstrated that ADMA induces the upregulation of ACE activity and the activation of AT1 receptor.[15] It is reasonably acceptable, therefore, that the ADMA/DDAH2 pathway exerts vascular action through multifaceted mechanisms involving NO, ROS, and Ang II/ACE. Of note, the dose of amlodipine used prevents the ADMA-induced elevation in blood pressure but fails to reduce vascular injury in WT mice (Figure 4) or ROS production (Figure 5A). We also found that hydralazine potently prevented the ADMA-induced hypertension, but had no effect on ROS generation (data not shown). It is highly likely therefore that blood pressure-independent factors, including ROS, mediate at least in part the ADMA-induced vascular injury.

The mechanism for the ACE upregulation by ADMA remains undetermined. Previous studies demonstrated that ACE protein expression was regulated by various mechanisms, including protein kinase C,[28] cyclic GMP,[29] cAMP,[30] and p38 MAPK.[31] It has also reported that p38 MAPK is activated by ADMA in HUVECs.[32] In the present study, we have observed that ADMA-induced upregulation of ACE is suppressed in HCAECs transfected with DDAH2 (Figure 8A). Furthermore, ADMA stimulates p38 MAP kinase and ACE protein expression, both of which are blocked by a specific p38MAP kinase inhibitor (SB203580), but not by a

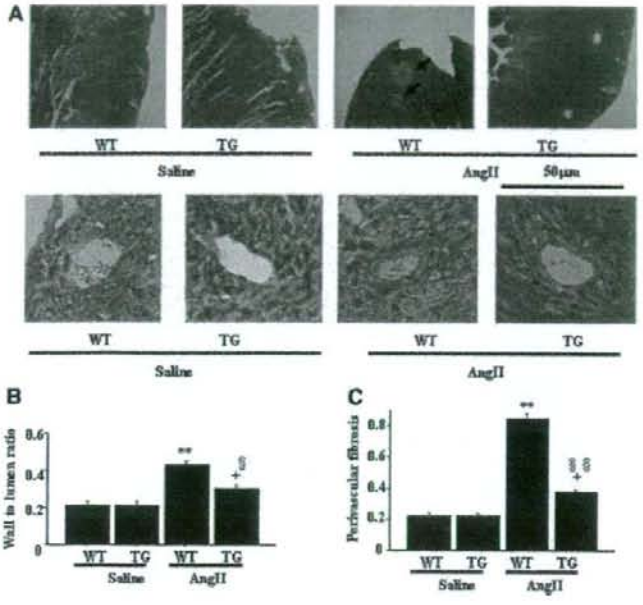

Figure 6. Effects of angiotensin II (Ang II) infusion on vascular lesions. A, In Masson-trichrome staining, Ang II caused marked vascular lesion in WT mice, but this effect was mitigated in TG mice. Upper panels show low power micrographs of the LV, whereas lower ones represent high power graphs. Lesions of coronary vascular beds were evaluated by wall to lumen ratio (B) and perivascular fibrosis (C). $^{**}P<0.01$ vs saline-infused WT mice, n=5. †$P<0.05$ vs saline-infused TG mice, n=5. §$P<0.05$ vs Ang II–infused WT mice, n=5. §§$P<0.01$ vs Ang II–infused WT mice, n=5.

p44/42 MAP kinase inhibitor (PD98059; Figure 8B, 8C). These findings therefore indicates that ADMA induces the expression of ACE through the activation of p38 MAP kinase.

Although Ang II is well documented as an important factor inducing vascular injury and subsequent organ damage, the role of the ADMA/DDAH2 pathway in mediating the Ang II–induced vascular injury has not been fully examined. It has been reported that the inhibition of Ang II action by the ACE inhibitor or the angiotensin receptor blocker decreases ADMA levels.[13,31] The present study shows that the Ang II–induced vascular injury is mitigated in mice overexpressing DDAH2, and this effect does not depend on systemic blood pressure (Figure 6). Furthermore, continuous infusion of Ang II elevates plasma ADMA levels in WT mice, but this effect is markedly suppressed in DDAH2 TG mice (Figure 7A). These observations allow speculation that ADMA mediates the Ang II–induced vascular injury, and in concert with the result showing ACE upregulation by ADMA (Figure 5B), there exists an intimate crosstalk between DDAH/ADMA and

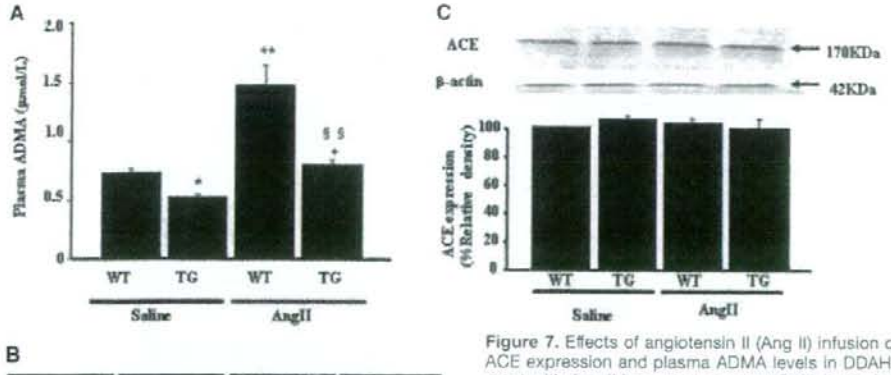

Figure 7. Effects of angiotensin II (Ang II) infusion on oxidative stress levels, ACE expression and plasma ADMA levels in DDAH2 TG mice. A, The treatment with Ang II increased plasma ADMA levels in WT mice. The increase in plasma ADMA levels were attenuated in TG mice. B, In dihydroethidium staining, WT mice with Ang II increased the cardiac fluorescent signals. In TG mice with Ang II, however, the treatment with Ang II did not augment the signals. C, Immunoblotting showed that Ang II infusion had no effects on ACE protein expression in heart homogenates of either WT or TG mice. $^{*}P<0.05$ vs saline-infused WT mice, n=5. $^{**}P<0.01$ vs saline-infused WT mice, n=5. †$P<0.05$ vs saline-infused TG mice, n=5. §§$P<0.01$ vs Ang II–infused WT mice, n=5.

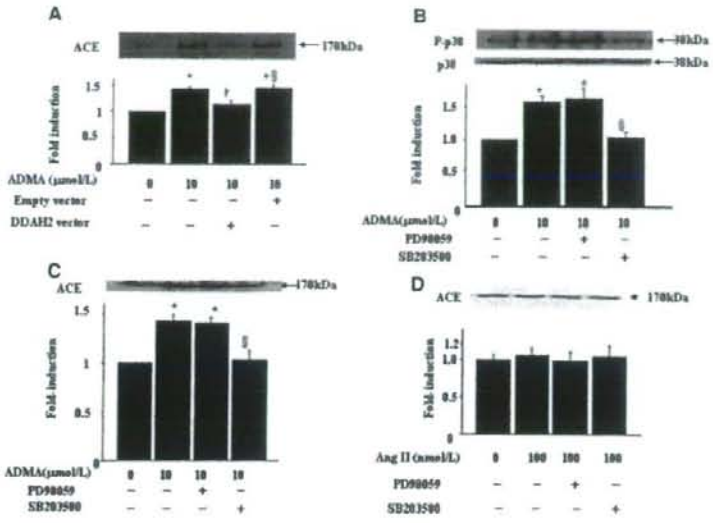

Figure 8. Effects of ADMA and Ang II on ACE expression and p38 MAPK actvity in HCAECs. A, ADMA (10μmol/L) directly induced the expresion of ACE, which was blocked by the DDAH2 overexpression. B, ADMA activated p38 MAPK, and this effect was prevented by a p38 MAP kinase inhibitor (SB203580), but not by a p44/42 MAP kinase inhibitor (PD98059). C, ADMA induced the ACE expression. This effect was blocked by p38 MAP kinase inhibition (SB203580). D, Ang II had no effect on the expression of ACE.

RAS. Of note, Ang II fails to upregulate ACE protein in mice (Figure 7C), and has no effect on ACE expression in cultured endothelial cells (Figure 8D). These observations could be explained by the different plasma ADMA levels reached in ADMA-infused (ie, 2.87±0.33 μmol/L) and Ang II–infused WT mice (ie, 1.48±0.15 μmol/L). Furthermore, the fact that the Ang II–induced vascular injury (Figure 6) or ROS production (Figure 7B) is not completely abolished in DDAH2 TG mice indicates that Ang II causes vascular injury through multiple mechanisms. Of greater importance, however, the current findings do indicate ADMA as a mediator of the Ang II–induced vascular injury.

The tentative mechanisms for the attenuation of ADMA-induced vascular damage in DDAH2 TG mice are illustrated in supplemental Figure I (available online at http://circres.ahajournals.org). ADMA activates p38 MAP kinase and upregulates the ACE expression in endothelial cells (ECs), which subsequently hydrolyzes Ang I to Ang II. Endogenous as well as exogenous Ang II activates NADPH oxidase and subsequently generates ROS in vascular smooth muscle cells.[34] ADMA also causes the inhibition of NOS, leading to decreased production of NO and overproduction of ROS. Because ROS is reported to inhibit DDAH,[35] Ang II could elevate ADMA production, which may contribute to the Ang II–induced vascular damage. Conversely, in DDAH2 TG mice, the overproduced ADMA is degraded, and the ADMA-associated vascular injury subsequently would be mitigated. This intriguing hypothesis however requires additional investigations.

In summary, the present study has demonstrated that the overexpression of DDAH2 reduces the ADMA level and affects tissue NO metabolism. DDAH2 overexpression prevents ADMA- and Ang II–induced vascular lesions, independently of systemic blood pressure. These effects are mainly mediated by the suppression of the ADMA-induced upregulation of local ACE or Ang II–induced oxidative stress. This mouse model therefore helps to understand both physiological and pathological relevance of the DDAH/ADMA pathway in the vascular tissue.

Sources of Funding

This work was supported by the Scientific Research Fund of the Ministry of Education, Culture, Sports, Science, and Technology of Japan (no. 18790624).

Disclosures

None.

References

1. Vallance P, Leone A, Calver A, Collier J, Moncada S. Accumulation of an endogenous inhibitor of nitric oxide synthesis in chronic renal failure. *Lancet*. 1992;339:572–576.
2. Boger RH, Bode-Boger SM, Szuba A, Tsao PS, Chan JR, Tangphao O, Blaschke TF, Cooke JP. Asymmetric dimethylarginine (ADMA): a novel risk factor for endothelial dysfunction: its role in hypercholesterolaemia. *Circulation*. 1998;98:1842–1847.
3. Zoccali C, bode-Boger S, Mallamaci F, Benedetto F, Tripepi G, Malatino L, Cataliotti A, Bellanuova I, Fermo I, Frolich J, Boger R. Plasma concentration of asymmetrical dimethylarginine and mortality in patients with end-stage renal disease: a prospective study. *Lancet*. 2001;358:2113–2117.
4. Leiper JM, Santa Maria J, Chubb A, MacAllister RJ, Charles IG, Whitley GS, Vallance P. Identification of two human dimethylarginine dimethylaminohydrolases with distinct tissue distributions and homology with microbial arginine deiminases. *Biochem J*. 1999;343:209–214.
5. MacAllister R, Parry H, Kimoto M, Ogawa T, Russell R, Hodson H, Whitley G, Vallance P. Regulation of nitric oxide synthesis by dimethylarginine dimethylaminohydrolase. *Br J Pharmacol*. 1996;119:1533–1540.
6. Chen Y, Li Y, Zhang P, Traverse JH, Hou M, Xu X, Kimoto M, Bache RJ. Dimethylarginine dimethylaminohydrolase and endothelial dysfunction in failing hearts. *Am J Physiol Heart Circ Physiol*. 2005;289:H2212–H2219.
7. Dayoub H, Achan V, Adimoolam S, Jacobi J, Stuehlinger MC, Wang BY, Tsao PS, Kimoto M, Vallance P, Patterson AJ, Cooke JP. Dimethylarginine dimethylaminohydrolase regulates nitric oxide synthesis: genetic and physiological evidence. *Circulation*. 2003;108:3042–3047.
8. Leiper J, Nandi M, Torondel B, Murray-Rust J, Malaki M, O'Hara B, Rossiter S, Anthony S, Madhani M, Selwood D, Smith C, Wojciak-Stothard B, Rudiger A, Stidwill R, McDonald NQ, Vallance P. Disruption of methylarginine metabolism impairs vascular homeostasis. *Nat Med*. 2007;13:198–203.

9. Jacobi J, Sydow K, von Degenfeld G, Zhang Y, Dayoub H, Wang B, Patterson AJ, Kimoto M, Blau HM, Cooke JP. Overexpression of dimethylarginine dimethylaminohydrolase reduces tissue asymmetric dimethylarginine levels and enhances angiogenesis. *Circulation*. 2005;111:1431–1438.
10. Tanaka M, Sydow K, Gunawan F, Jacobi J, Tsao PS, Robbins RC, Cooke JP. Dimethylarginine dimethylaminohydrolase overexpression suppresses graft coronary artery disease. *Circulation*. 2005;112:1549–1556.
11. Ito A, Tsao PS, Adimoolam S, Kimoto M, Ogawa T, Cooke JP. Novel mechanism for endothelial dysfunction: dysregulation of dimethylarginine dimethylaminohydrolase. *Circulation*. 1999;99:3092–3095.
12. Lin KY, Ito A, Asagami T, Tsao PS, Adimoolam S, Kimoto M, Tsuji H, Reaven GM, Cooke JP. Impaired nitric oxide synthase pathway in diabetes mellitus: role of asymmetric dimethylarginine and dimethylarginine dimethylaminohydrolase. *Circulation*. 2002;106:987–992.
13. Jiang JL, Zhu HQ, Chen Z, Xu HY, Li YJ. Angiotensin-converting enzyme inhibitors prevent LDL-induced endothelial dysfunction by reduction of asymmetric dimethylarginine level. *Int J Cardiol*. 2005;101:153–155.
14. Napoli C, Sica V, de Nigris F, Pignalosa O, Condorelli M, Ignarro LJ, Liguori A. Sulfhydryl angiotensin-converting enzyme inhibition induces sustained reduction of systemic oxidative stress and improves the nitric oxide pathway in patients with essential hypertension. *Am Heart J*. 2004;148:e5.
15. Suda O, Tsutsui M, Morishita T, Tasaki H, Ueno S, Nakata S, Tsujimoto T, Toyohira Y, Hayashida Y, Sasaguri Y, Ueta Y, Nakashima Y, Yanagihara N. Asymmetric dimethylarginine produces vascular lesions in endothelial nitric oxide synthase-deficient mice: involvement of renin-angiotensin system and oxidative stress. *Arterioscler Thromb Vasc Biol*. 2004;24:1682–1688.
16. Hasegawa K, Wakino S, Tanaka T, Kimoto M, Tatematsu S, Kanda T, Yoshioka K, Homma K, Sugano N, Kurabayashi M, Saruta T, Hayashi K. Dimethylarginine dimethylaminohydrolase 2 increases vascular endothelial growth factor expression through Sp1 transcription factor in endothelial cells. *Arterioscler Thromb Vasc Biol*. 2006;26:1488–1494.
17. Chuma S, Nakatsuji N. Autonomous transition into meiosis of mouse fetal germ cells in vitro and its inhibition by gp130-mediated signaling. *Dev Biol*. 2001;229:468–479.
18. Hasegawa K, Nakatsuji N. Insulators prevent transcriptional interference between two promoters in a double gene construct for transgenesis. *FEBS Lett*. 2002;520:47–52.
19. Tsao PS, McEvoy LM, Drexler H, Butcher EC, Cooke JP. Enhanced endothelial adhesiveness in hypercholesterolemia is attenuated by L-arginine. *Circulation*. 1994;89:2176–2182.
20. Azumi H, Inoue N, Ohashi Y, Terashima M, Mori T, Fujita H, Awano K, Kobayashi K, Maeda K, Hata K, Shinke T, Kobayashi S, Hirata K, Kawashima S, Itabe H, Hayashi Y, Imajoh-Ohmi S, Itoh H, Yokoyama M. Superoxide generation in directional coronary atherectomy specimens of patients with angina pectoris: important role of NAD(P)H oxidase. *Arterioscler Thromb Vasc Biol*. 2002;22:1838–1844.
21. Wakino S, Kintscher U, Liu Z, Kim S, Yin F, Ohba M, Kuroki T, Schonthal AH, Hsueh WA, Law RE. Peroxisome proliferator-activated receptor gamma ligands inhibit mitogenic induction of p21(Cip1) by modulating the protein kinase Cdelta pathway in vascular smooth muscle cells. *J Biol Chem*. 2001;276:47650–47657.
22. Cole JM, Khokhlova N, Sutliff RL, Adams JW, Disher KM, Zhao H, Capecchi MR, Corvol P, Bernstein KE. Mice lacking endothelial ACE: normal blood pressure with elevated angiotensin II. *Hypertension*. 2003;41:313–321.
23. Li D, Singh RM, Liu L, Chen H, Singh BM, Kazzaz N, Mehta JL. Oxidized-LDL through LOX-1 increases the expression of angiotensin converting enzyme in human coronary artery endothelial cells. *Cardiovasc Res*. 2003;57:238–243.
24. Miyazaki H, Matsuoka H, Cooke JP, Usui M, Ueda S, Okuda S, Imaizumi T. Endogenous nitric oxide synthase inhibitor: a novel marker of atherosclerosis. *Circulation*. 1999;99:1141–1146.
25. Abbasi F, Asagmi T, Cooke JP, Lamendola C, McLaughlin T, Reaven GM, Stuehlinger M, Tsao PS. Plasma concentrations of asymmetric dimethylarginine are increased in patients with type 2 diabetes mellitus. *Am J Cardiol*. 2001;88:1201–1203.
26. Boger RH, Bode-Boger SM, Tsao PS, Lin PS, Chan JR, Cooke JP. An endogenous inhibitor of nitric oxide synthase regulates endothelial adhesiveness for monocytes. *J Am Coll Cardiol*. 2000;36:2287–2295.
27. Sydow K, Munzel T. ADMA and oxidative stress. *Atheroscler Suppl*. 2003;4:41–51.
28. Villard E, Alonso A, Agrapart M, Challah M, Soubrier F. Induction of angiotensin I-converting enzyme transcription by a protein kinase C-dependent mechanism in human endothelial cells. *J Biol Chem*. 1998;273:25191–25197.
29. Saijonmaa O, Fyhrquist F. Upregulation of angiotensin converting enzyme by atrial natriuretic peptide and cyclic GMP in human endothelial cells. *Cardiovasc Res*. 1998;40:206–210.
30. Xavier-Neto J, Pereira AC, Junqueira ML, Carmona R, Krieger JE. Rat angiotensin-converting enzyme promoter regulation by beta-adrenergics and cAMP in endothelium. *Hypertension*. 1999;34:31–38.
31. Saijonmaa O, Nyman T, Fyhrquist F. Downregulation of angiotensin-converting enzyme by tumor necrosis factor-alpha and interleukin-1beta in cultured human endothelial cells. *J Vasc Res*. 2001;38:370–378.
32. Jiang DJ, Jia SJ, Dai Z, Li YJ. Asymmetric dimethylarginine induces apoptosis via p38 MAPK/caspase-3-dependent signaling pathway in endothelial cells. *J Mol Cell Cardiol*. 2006;40:529–539.
33. Ito A, Egashira K, Narishige T, Muramatsu K, Takeshita A. Angiotensin-converting enzyme activity is involved in the mechanism of increased endogenous nitric oxide synthase inhibitor in patients with type 2 diabetes mellitus. *Circ J*. 2002;66:811–815.
34. Seshiah PN, Weber DS, Rocic P, Valppu L, Taniyama Y, Griendling KK. Angiotensin II stimulation of NAD(P)H oxidase activity: upstream mediators. *Circ Res*. 2002;91:406–441.
35. Leiper J, Murray-Rust J, McDonald N, Vallance P. S-nitrosylation of dimethylarginine dimethylaminohydrolase regulates enzyme activity. *Proc Natl Acad Sci U S A*. 2002;99:13527–13532.

Original Article

(Pro)Renin Receptor–Mediated Activation of Mitogen-Activated Protein Kinases in Human Vascular Smooth Muscle Cells

Mariyo SAKODA[1], Atsuhiro ICHIHARA[1], Yuki KANESHIRO[1], Tomoko TAKEMITSU[1], Yuichi NAKAZATO[2], A.H.M. Nurun NABI[3], Tsutomu NAKAGAWA[4], Fumiaki SUZUKI[3),4)], Tadashi INAGAMI[5], and Hiroshi ITOH[1]

Blockade of (pro)renin receptor has benefits in diabetic angiotensin II type-1a-receptor–deficient mice, suggesting the importance of (pro)renin receptor–mediated intracellular signals. To determine the mechanism whereby the human (pro)renin receptor activates mitogen-activated protein kinases in human vascular smooth muscle cells (hVSMC), we treated the cells with recombinant human prorenin. Prorenin enhanced hVSMC proliferation and activated extracellular-signal–related protein kinase (ERK) in a dose- and time-dependent manner but did not influence activation of p38 or c-Jun NH_2-terminal kinase. The activated ERK level was reduced to the control level by the tyrosine kinase inhibitor genistein, and the MEK inhibitor U0126 markedly reduced the activated ERK level to the control level, whereas the level of activated ERK was unaffected by the angiotensin-converting enzyme inhibitor imidaprilat or the angiotensin II receptor blocker candesartan. A human (pro)renin receptor was present in hVSMCs, and its knockdown with small interfering RNA (siRNA) significantly inhibited the prorenin-induced ERK activation. These results suggest that prorenin stimulates ERK phosphorylation in hVSMCs through the receptor-mediated activation of tyrosine kinase and subsequently MEK, independently of the generation of angiotensin II or the activation of its receptor. The (pro)renin receptor–mediated ERK signal transduction is thus a possible new therapeutic target for preventing vascular complications. (*Hypertens Res* 2007; 30: 1139–1146)

***Key Words*: extracellular-signal–related protein kinase, prorenin, receptor, small interfering RNA, vascular smooth muscle cells**

Introduction

Binding of prorenin to an intrinsic prorenin-binding receptor plays an important role in the development of cardiovascular complications in hypertension and diabetes, such as cardiac fibrosis (*1*), nephrosclerosis (*2*), and microvascular complications (*3*, *4*). These effects have been considered to be mediated by the receptor-associated prorenin (RAP) system and consist of two major pathways: activation of the renin-angiotensin system (RAS) by conversion of prorenin to its active form by a conformational change instead of proteolytic cleavage of the prosegment of prorenin (*3*, *5*), and stimulation of the RAS-independent intracellular pathways *via* the

From the [1]Department of Internal Medicine, Keio University School of Medicine, Tokyo, Japan; [2]Saitama Social Insurance Hospital, Saitama, Japan; [3]United Graduate School of Agricultural Science and [4]Faculty of Applied Biological Sciences, Gifu University, Gifu, Japan; and [5]Biochemistry, Vanderbilt University School of Medicine, Nashville, USA.

This work was supported in part by a Grant-in-Aid for Scientific Research from the Ministry of Education, Culture, Sports, Science and Technology of Japan (17390249) and by a grant from NHLBI (HL58205).

Address for Reprints: Atsuhiro Ichihara, M.D., Ph.D., Department of Internal Medicine, Keio University School of Medicine, 35 Shinanomachi, Shinjuku-ku, Tokyo 160–8582, Japan. E-mail: atzichi@sc.itc.keio.ac.jp

Received March 30, 2007; Accepted in revised form June 25, 2007.

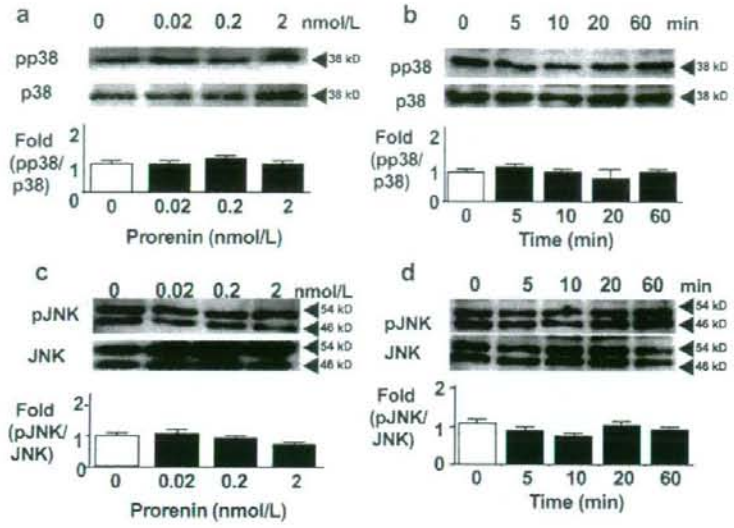

Fig. 1. *Dose response and time course of activation of p38 (a and b, respectively) and c-Jun NH_2-terminal kinase (JNK, c and d, respectively) after addition of human recombinant prorenin to human vascular smooth muscle cells (VSMCs; n = 5 in each). Representative Western blots are presented. The relative density of phosphorylated p38 (pp38) to p38 or phosphorylated JNK (pJNK) to JNK is shown in the bar graphs. Neither p38 nor JNK was stimulated by prorenin in human VSMCs.*

(pro)renin receptor (*5–8*).

Studies using cultured mesangial cells have provided evidence that stimulation of the (pro)renin receptor caused activation of extracellular-signal–related protein kinases (ERK) (*5*) and stimulation of transforming growth factor-β expression (*7*) through a RAS-independent mechanism. More recently, prorenin-treated cardiomyocytes showed stimulation of p38, but not ERK, through an angiotensin II–independent mechanism (*9*). Since RAP-dependent, RAS-independent activation of all three members of the mitogen-activated protein kinase (MAPK) family, including ERK, p38, and c-Jun NH_2-terminal kinase (JNK), was observed in the kidneys of diabetic mice (*8*), RAP-mediated intracellular signal transduction may depend on cell types. However, the signaling mechanisms of the (pro)renin receptor in vascular smooth muscle cells (VSMCs) have remained unclear despite the significant presence of this receptor in the small arteries (*5*).

The present study was designed to determine the involvement of the three members of the MAPK family in the (pro)renin receptor–mediated intracellular signal transduction in human VSMCs. Targeting of the (pro)renin receptor signal independent of angiotensin II receptor activation may provide a new therapeutic strategy for vascular complications in hypertension and diabetes.

Methods

Reagents

U0126, an MEK inhibitor, and genistain, a tyrosine kinase inhibitor, were purchased from A.G. Scientific Inc. (San Diego, USA) and Sigma (St. Louis, USA), respectively. Imidaprilat, an angiotensin-converting enzyme (ACE) inhibitor, and candesartan (CV11974), an angiotensin II type 1 receptor blocker (ARB), were kindly provided by Tanabe Seiyaku Co. (Osaka, Japan) and Takeda Chemical Industry (Osaka, Japan), respectively.

Prorenin Actions on Human VSMCs

Recombinant human prorenin was prepared from Chinese hamster ovary cell lines harboring human prorenin cDNA (*10*). Human VSMCs were obtained from Cell Systems (Kirkland, USA) and grown in Dulbecco's Modified Eagle's Medium (DMEM; Sigma) supplemented with 10% fetal calf serum according to the manufacturer's instructions. Experiments were performed with VSMCs maintained in culture for 4 to 10 passages. Before the experiments, cells were exposed to serum-free medium for 24 h. The cells were treated with human recombinant prorenin in a dose-dependent and time-dependent manner and then harvested for the measurement of

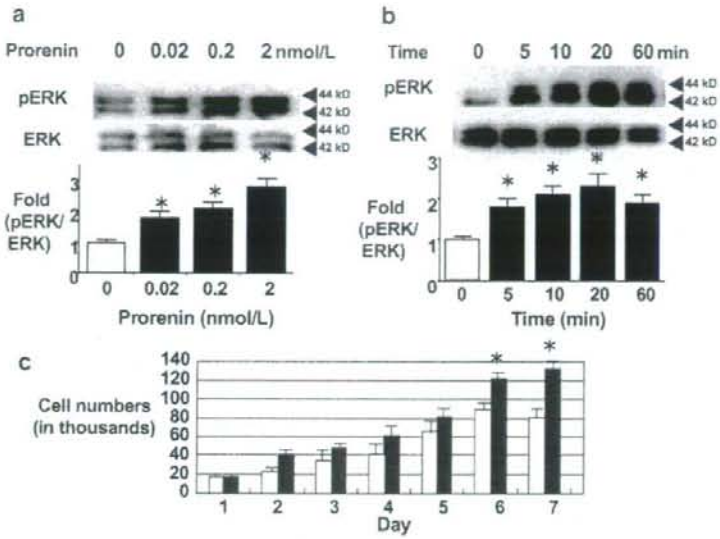

Fig. 2. *Extracellular-signal–related protein kinase (ERK) activation and growth by human recombinant prorenin in human vascular smooth muscle cells (VSMCs). a: The dose response was determined at 20 min after the addition of prorenin (n = 4), and b: the time course in response to 2 nmol/L prorenin was assessed (n = 4). Representative Western blots are presented. The relative density of phosphorylated ERK (pERK) to ERK is shown in the bar graphs. *p < 0.05 vs. the control. The stimulation of ERK (pERK) was dose-dependent and peaked at 20 min. c: Untreated human VSMCs (open bar; n = 3) and human VSMCs treated with 2 nmol/L human recombinant prorenin (closed bar; n = 3) were counted in triplicate once daily for 7 days by flow cytometry. *p < 0.05 vs. untreated VSMCs.*

(pro)renin receptor mRNA and ERK protein. Proliferation of VSMCs was determined by cell counts performed in triplicate once daily for 7 days with the use of a flow cytometer (Epics XL; Beckman Coulter, Fullerton, USA). Experiments were performed in the presence and absence of mannose-6-phosphate in the medium, but similar results were obtained.

MAPK Western Blot Analysis

Western blot analyses were performed as reported previously (*11, 12*). Briefly, cultured human VSMCs were lysed in lysis buffer containing Tris (50 mmol/L), NaCl (100 mmol/L), NAF (50 mmol/L), EDTA (1 mmol/L), 0.1% sodium dodecyl sulfate (SDS), 0.5% deoxycholic acid sodium salt, 1% Triton X-100 and protease inhibitor (1 tab/9 mL buffer). Following centrifugation at 15,000 rpm for 15 min at 4°C, the supernatant was collected and subjected to SDS polyacrylamide gel electrophoresis. The proteins were transferred to polyvinylidene difluoride membranes, and after blocking the blots for 1 h with TBS-T containing 5% bovine serum albumin and 0.5% Tween 20, they were incubated for 24 h with mouse monoclonal anti-phosphorylated ERK antibody (1:1,000 dilution; Cell Signaling Technology, Beverly, USA), mouse monoclonal anti-ERK antibody (1:1,000 dilution; Cell Signaling Technology), mouse monoclonal anti-phosphorylated JNK antibody (1:500 dilution; Santa Cruz Biotechnology, Santa Cruz, USA), rabbit polyclonal anti-JNK antibody (1:1,000 dilution; Santa Cruz Biotechnology), mouse monoclonal anti-phosphorylated p38 antibody (1:500 dilution; Santa Cruz Biotechnology), or rabbit polyclonal anti-p38 antibody (1:1,000 dilution; Santa Cruz Biotechnology). Immunoreactivity was detected by horseradish-peroxidase–conjugated donkey anti-mouse antibody and an enhanced chemiluminescence reaction, and the quantitative analyses were performed with Image 1D (Pharmacia, Peapack, USA).

RNA Preparation and Real-Time Reverse Transcription–Polymerase Chain Reaction of the (Pro)Renin Receptor

Total RNA was extracted from human VSMCs with an RNeasy Mini Kit (QIAGEN, Tokyo, Japan), and a real-time quantitative reverse transcription–polymerase chain reaction (RT-PCR) was performed with the TaqMan One-Step RT-PCR Master Mix Reagents Kit, an ABI Prism 7700 HT Detection System (Applied Biosystems, Foster City, USA). We designed the probes and primers for the human (pro)renin receptor (forward, 5′-AGATGACATGTACAGTCTTTATG

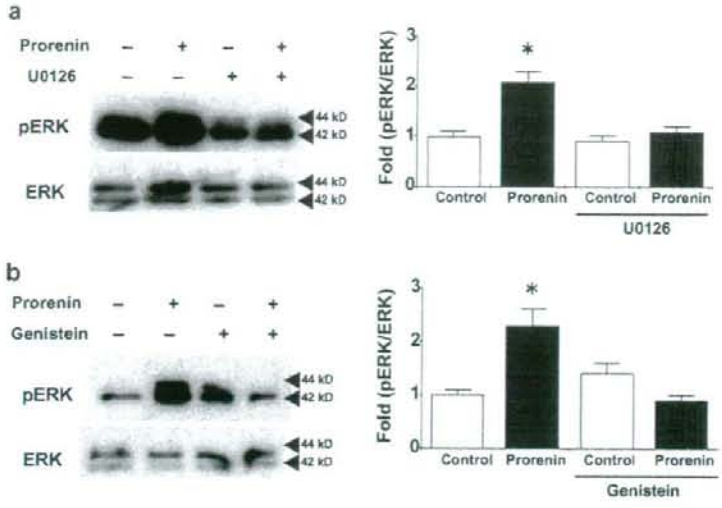

Fig. 3. *Extracellular-signal–related protein kinase (ERK) activation at 20 min after the addition of 2 nmol/L human prorenin in the presence and absence of 20 nmol/L U0126, an MEK inhibitor (n = 5; a) or 100 μmol/L genistain, a tyrosine kinase inhibitor (n = 5; b). Data are presented as a representative Western blots obtained from the experiments. The relative density of phosphorylated ERK (pERK) to ERK is presented in the bar graphs. ERK activation was completely blocked by U0126 or genistein. *p < 0.05 vs. the control.*

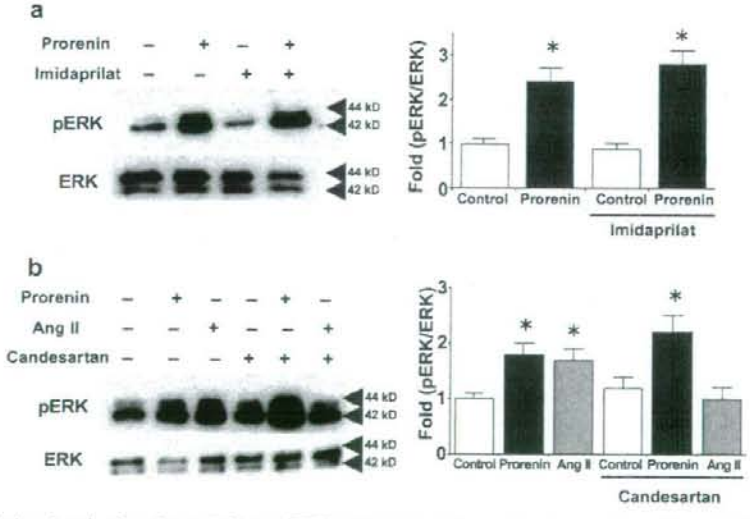

Fig. 4. *Extracellular-signal–related protein kinase (ERK) activation at 20 min after the addition of 2 nmol/L human prorenin or 1 μmol/L angiotensin (Ang) II in the presence and absence of 10 μmol/L imidaprilat, an ACE inhibitor (n = 5; a) or 10 μmol/L candesartan, an angiotensin II type 1 receptor blocker (n = 5; b). Data are presented as representative Western blots. The relative density of phosphorylated ERK (pERK) to ERK is given in the bar graphs. *p < 0.05 vs. the control. Neither imidapril nor candesartan inhibited prorenin stimulation of ERK.*

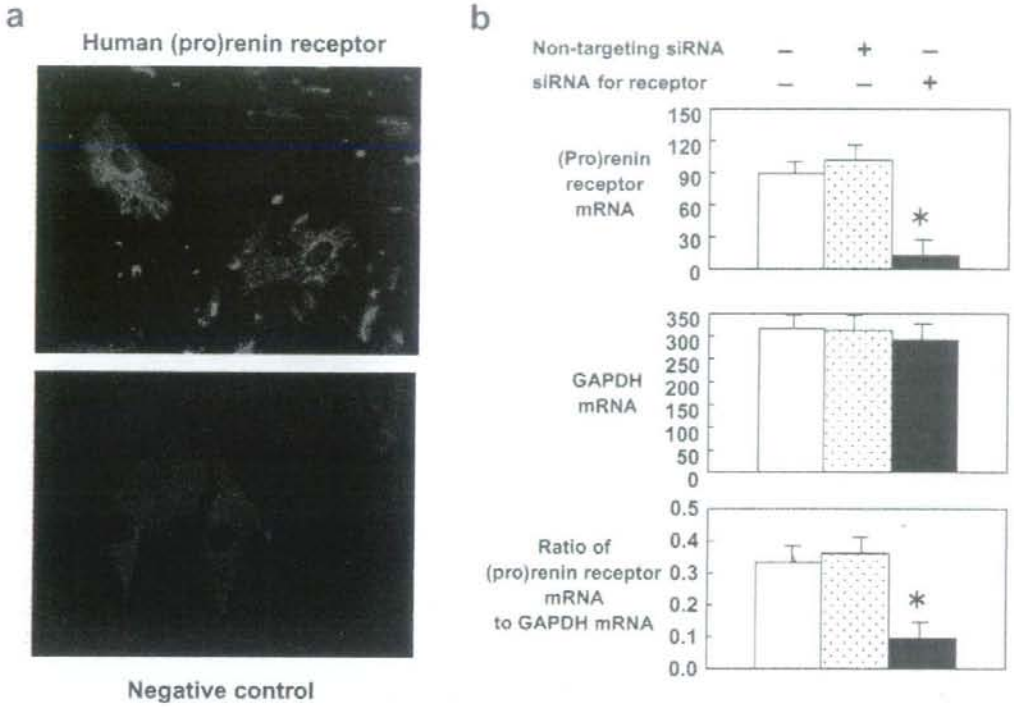

Fig. 5. *Photomicrograph of immunocytochemistry for human (pro)renin receptor (a) and effects of siRNA on human (pro)renin receptor mRNA (b) in human vascular smooth muscle cells. Targeting siRNA, but not control non-targeting siRNA, significantly decreased (pro)renin receptor mRNA expression as determined by real-time RT-PCR analysis for human (pro)renin receptor mRNA (n=5). *$p<0.05$ vs. untreated cells and cells treated with non-targeting siRNA.*

GTGG-3′; reverse, 5′-TGCTGGGTTCTTCGCTTGT-3′; probe, 5′-FAM-TTTGACACCTCCCTCATTAGGAAGAC AAGGACT-TAMRA-3′) and GAPDH (forward, 5′-TGACA ACTCCCTCAAGATTGTCA-3′; reverse, 5′-GGCATGGAC TGTGGTCATGA-3′; probe, 5′-FAM-TGCATCCTGCACC ACCAACTGCTTAG-TAMRA-3′), based on its previously reported cDNA sequence (5).

Silencing the Human (Pro)Renin Receptor

Human (pro)renin receptor mRNA was specifically knocked down using commercially available small interfering RNA (siRNA) oligonucleotides for ATP6AP2 (Dharmacon, Lafayette, USA). Before transfection, human VSMCs were maintained in DMEM with 10% fetal calf serum and then transfected with Dharmafect™ (Dharmacon), and the human (pro)renin receptor siRNA according to the manufacturer's instructions. Scrambled non-targeting siRNA was used as control.

Immunofluorescence Labeling for the (Pro)Renin Receptor

Cells were fixed with 4% paraformaldehyde and incubated in 100% methanol at −20°C for 10 min. After washing three times in PBS, the cells were incubated with the goat polyclonal anti-ATP6IP2 antibody (1:200 dilution; Abcam Inc., Cambridge, USA). After washing in PBS, the sections were incubated with TRITC-conjugated donkey anti-goat IgG (1:200 dilution; Molecular Probes Inc., Eugene, USA). Slides were examined with a Zeiss confocal microscope.

Statistical Analyses

Statistical comparisons were made by using two-way ANOVA and the Fisher's exact test. Values of $p<0.05$ were considered to indicate statistical significance. Data are reported as the means±SEM. Duplicate wells were analyzed for each experiment, and each experiment was performed independently at least five times.

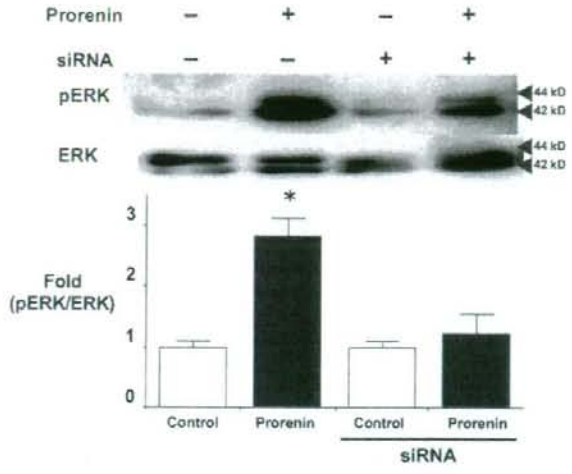

Fig. 6. *Effects of siRNA for human (pro)renin receptor mRNA on extracellular-signal-related protein kinase (ERK) activation at 20 min after the addition of 2 nmol/L human prorenin (n=5). Data are presented as a representative Western blots. The relative density of phosphorylated ERK (pERK) to ERK is given in the bar graph. *p<0.05 vs. the control. The siRNA, which reduced (pro)renin receptor expression to the control level, markedly inhibited ERK activation to an insignificant level.*

Results

Effects of Human Prorenin on MAPK Activation and Proliferation of Human VSMCs

Human recombinant prorenin did not affect the activation of JNK or p38 in human VSMCs ($n=5$) at any doses or incubation periods used in the present study (Fig. 1). However, human recombinant prorenin-treated human VSMCs ($n=4$) showed dose-dependent progressive increases in ERK phosphorylation (Fig. 2a). A 2.7-fold increase in ERK activation was observed 20 min following the addition of 2 nmol/L prorenin, which was the highest concentration of prorenin used in the present study. A time-dependent increase in ERK activation was also seen, with a 2.3-fold maximum increase at the 20 min interval ($n=4$; Fig. 2b). Significantly greater proliferation was seen in VSMCs treated with 2 nmol/L prorenin than in untreated VSMCs ($n=3$ in each; Fig. 2c). After 7 days in culture, the average number of VSMCs in the culture treated with prorenin was 1.6-fold greater than that in untreated VSMCs. The human prorenin–induced ERK activation was completely blocked by treatment with either the MEK inhibitor U0126 or the tyrosine kinase inhibitor genistein ($n=5$ in each; Fig. 3).

The Effects of Prorenin Were Independent of Angiotensin II Generation

We examined whether angiotensin II generated by non-proteolytic activation of prorenin *(13)* contributes to the prorenin-induced activation of ERK in human VSMCs ($n=5$). In the presence of the ACE inhibitor imidaprilat, prorenin significantly increased the ERK activation in human VSMCs, and the increase (2.8-fold) was similar to the 2.4-fold increase in the absence of imidaprilat (Fig. 4a). Treatment with the ARB candesartan significantly inhibited the ERK activation caused by angiotensin II but had no effect on the prorenin-induced activation of ERK in human VSMCs ($n=5$; Fig. 4b). The presence or absence of candesartan did not significantly affect the prorenin-induced ERK activation, with the average increases being 1.8- and 2.2-fold, respectively. The results indicate that the prorenin-induced activation of ERK was independent of angiotensin II in human VSMCs.

Presence and Role of the (Pro)Renin Receptor in Human VSMCs

To determine whether prorenin-induced ERK activation is mediated by the (pro)renin receptor, we measured the presence of human (pro)renin receptor mRNA and protein in human VSMCs (Fig. 5). Further, we showed that transfection of an siRNA targeting the (pro)renin receptor induced a significant decrease in receptor mRNA ($n=5$). Treatment of cells with Dharmafect or non-targeting control siRNA did not

affect (pro)renin receptor mRNA expression. Human VSMCs transfected for 24 h with 100 nmol/L siRNA molecules had no detectable (pro)renin receptor mRNA and showed significantly reduced induction of ERK activation with prorenin treatment (n=5: Fig. 6), suggesting that the human VSMC (pro)renin receptor mediates prorenin-induced activation of ERK.

Discussion

Binding of prorenin to the (pro)renin receptor promotes two mechanisms: activation of the RAS by non-proteolytic activation of prorenin and stimulation of the RAS-independent pathways emanating from the (pro)renin receptor (*14*). The present study clearly showed that recombinant human prorenin stimulated activation of ERK, but not p38 or JNK, independently of angiotensin II in human VSMCs, though it is well known that activation of type 1 angiotensin II receptor leads to phosphorylation of ERK in a variety of cells (*15, 16*). Nonetheless, the prorenin-induced activation of ERK was here found to be dependent on tyrosine kinase(s) and MEK.

The ERK cascade is involved in the regulation of cell differentiation and proliferation by G-protein–coupled receptors. Once activated, ERK can translocate to the nucleus, where it is thought to regulate the expression of transcription factors, and thereby regulate cell differentiation and proliferation (*17*). In the present study, the (pro)renin receptor was present in human VSMCs, and VSMC proliferation was enhanced in its presence. In addition, a recent study demonstrated that hypertension develops in transgenic rats overexpressing the human (pro)renin receptor specifically in smooth muscle cells (*18*). This finding suggests that the (pro)renin receptor–mediated ERK activation in VSMCs may be involved in a vascular remodeling which induces an increase in peripheral vascular resistance, leading to the development of hypertension. However, the vascular remodeling process is caused by an imbalance between growth and apoptosis of VSMCs. Thus, further *in vivo* studies will be needed to clarify whether the (pro)renin receptor–mediated, angiotensin II–independent ERK activation stimulates the growth, inhibits the apoptosis, or both.

In cultured mesangial cells, renin/prorenin has been reported to stimulate activation of ERK (*5*) and expression of transforming growth factor-β (*7*) through a RAS-independent mechanism. Since the angiotensinogen-deficient mice have high prorenin levels in the juxtaglomerular area of the kidneys and develop glomerulosclerosis (*19*), stimulation of the (pro)renin receptor by prorenin can contribute to the development of angiotensin II–independent glomerulosclerosis. Likewise, the transgenic rats overexpressing rat prorenin specifically in the liver had high plasma prorenin levels with no increase in plasma renin activity or plasma angiotensinogen levels and developed arterial wall thickening and aortic wall hypertrophy without hypertension (*20*). Since the present study found that prorenin stimulates the activation of ERK in VSMCs, high plasma prorenin levels can stimulate the VSMC (pro)renin receptor and thereby cause cell proliferation independently of the activity of angiotensin II.

In conclusion, human prorenin caused a phosphorylation of ERK through angiotensin II–independent, (pro)renin receptor–mediated activation of tyrosine kinase and subsequent MEK in human VSMCs. Although further *in vivo* studies are needed to determine whether the prorenin effects observed in the present study play a role in development and progression of atherosclerosis, the results of the present study raise the possibility that the RAP system is a novel therapeutic target for atherosclerosis.

Acknowledgements

We thank Ms. Ai Fukushima and Ms. Kumi Satoh for their excellent technical assistance.

References

1. Ichihara A, Kaneshiro Y, Takemitsu T, *et al*: Non-proteolytic activation of prorenin contributes to development of cardiac fibrosis in genetic hypertension. *Hypertension* 2006; **47**: 894–900.
2. Ichihara A, Kaneshiro Y, Takemitsu T, *et al*: Contribution of non-proteolytically activated prorenin in glomeruli to hypertensive renal damage. *J Am Soc Nephrol* 2006; **17**: 2495–2503.
3. Ichihara A, Hayashi M, Kaneshiro Y, *et al*: Inhibition of diabetic nephropathy by a decoy peptide corresponding to the "handle" region for non-proteolytic activation of prorenin. *J Clin Invest* 2004; **114**: 1128–1135.
4. Satofuka S, Ichihara A, Nagai N, *et al*: Suppression of ocular inflammation in endotoxin-induced uveitis by inhibiting nonproteolytic activation of prorenin. *Invest Ophthalmol Vis Sci* 2006; **47**: 2686–2692.
5. Nguyen G, Delarue F, Burckle C, *et al*: Pivotal role of the renin/prorenin receptor in angiotensin II production and cellular responses to renin. *J Clin Invest* 2002; **109**: 1417–1427.
6. Schefe J, Funke-Kaiser H, Jost A, *et al*: Signal transduction of the renin/prorenin receptor. *J Hypertens* 2005; **23**: S354 (Abstract).
7. Huang Y, Wongamorntham S, Kasting J, *et al*: Renin increases mesangial cell transforming growth factor-β1 and matrix proteins through receptor-mediated angiotensin II–independent mechanisms. *Kidney Int* 2006; **69**: 105–113.
8. Ichihara A, Suzuki F, Nakagawa T, Kaneshiro Y, *et al*: Prorenin receptor blockade inhibits development of glomerulosclerosis in diabetic angiotensin II type 1a receptor deficient mice. *J Am Soc Nephrol* 2006; **17**: 1950–1961.
9. Saris J, 't Hoen P, Garrelds I, *et al*: Prorenin induces intracellular signaling in cardiomyocytes independently of angiotensin II. *Hypertension* 2006; **48**: 564–571.
10. Poorman R, Palermo D, Post L, *et al*: Isolation and characterization of native human renin derived from Chinese hamster ovary cells. *Proteins* 1986; **1**: 139–145.
11. Li P-G, Xu J-W, Ikeda K, *et al*: Caffeic acid inhibits vascu-

lar smooth muscle cell proliferation induced by angiotensin II in stroke-prone spontaneously hypertensive rats. *Hypertens Res* 2005; **28**: 369–377.
12. Kaneshiro Y, Ichihara A, Takemitsu T, *et al*: Increased expression of cyclooxygenase-2 in renal cortex of human-prorenin-receptor–gene transgenic rats. *Kidney Int* 2006; **70**: 641–646.
13. Suzuki F, Hayakawa M, Nakagawa T, *et al*: Human prorenin has "gate and handle" regions for its non-proteolytic activation. *J Biol Chem* 2003; **278**: 22217–22222.
14. Catanzaro DF: Physiological relevance of renin/prorenin binding and uptake. *Hypertens Res* 2005; **28**: 97–105.
15. Eguchi S, Inagami T: Signal transduction of angiotensin II type 1 receptor through receptor tyrosine kinase. *Regul Pept* 2000; **91**: 13–20.
16. Li P-G, Xu J-W, Ikeda K, *et al*: Caffeic acid inhibits vascular smooth muscle cell proliferation induced by angiotensin II in stroke-prone spontaneously hypertensive rats. *Hypertens Res* 2005; **28**: 369–377.
17. Marshall C: Specificity of receptor tyrosine kinase signaling: transient *versus* sustained extracellular signal–regulated kinase activation. *Cell* 1995; **80**: 179–185.
18. Burckle C, Jan Danser A, Muller D, *et al*: Elevated blood pressure and heart rate in human renin receptor transgenic rats. *Hypertension* 2006; **47**: 1–5.
19. Niimura F, Labosky P, Kakuchi J, *et al*: Gene targeting in mice reveals a requirement for angiotensin in the development and maintenance of kidney morphology and growth factor regulation. *J Clin Invest* 1995; **96**: 2947–2954.
20. Veniant M, Menard J, Bruneval P, *et al*: Vascular damage without hypertension in transgenic rats expressing prorenin exclusively in the liver. *J Clin Invest* 1996; **98**: 1966–1970.

Adrenomedullin/Cyclic AMP Pathway Induces Notch Activation and Differentiation of Arterial Endothelial Cells From Vascular Progenitors

Takami Yurugi-Kobayashi, Hiroshi Itoh, Timm Schroeder, Akiko Nakano, Genta Narazaki, Fumiyo Kita, Kentoku Yanagi, Mina Hiraoka-Kanie, Emi Inoue, Toshiaki Ara, Takashi Nagasawa, Ursula Just, Kazuwa Nakao, Shin-Ichi Nishikawa, Jun K. Yamashita

Objective—The acquisition of arterial or venous identity is highlighted in vascular development. Previously, we have reported an embryonic stem (ES) cell differentiation system that exhibits early vascular development using vascular endothelial growth factor (VEGF) receptor-2 (VEGFR2)-positive cells as common vascular progenitors. In this study, we constructively induced differentiation of arterial and venous endothelial cells (ECs) in vitro to elucidate molecular mechanisms of arterial-venous specification.

Methods and Results—ECs were induced from VEGFR2$^+$ progenitor cells with various conditions. VEGF was essential to induce ECs. Addition of 8bromo-cAMP or adrenomedullin (AM), an endogenous ligand-elevating cAMP, enhanced VEGF-induced EC differentiation. Whereas VEGF alone mainly induced venous ECs, 8bromo-cAMP (or AM) with VEGF supported substantial induction of arterial ECs. Stimulation of cAMP pathway induced Notch signal activation in ECs. The arterializing effect of VEGF and cAMP was abolished in recombination recognition sequence binding protein at the Jκ site deficient ES cells lacking Notch signal activation or in ES cells treated with γ-secretase inhibitor. Nevertheless, forced Notch activation by the constitutively active Notch1 alone did not induce arterial ECs.

Conclusions—Adrenomedullin/cAMP is a novel signaling pathway to activate Notch signaling in differentiating ECs. Coordinated signaling of VEGF, Notch, and cAMP is required to induce arterial ECs from vascular progenitors. (***Arterioscler Thromb Vasc Biol.* 2006;26:1977-1984.**)

Key Words: angiogenesis ■ developmental biology ■ embryonic stem cells ■ endothelium ■ vascular biology

Vascular formation is a complicated but well-organized process that involves sprouting, branching, and differential growth of vessels from the primary plexus or existing vessels into a functioning circulation system.[1] During the process, vascular cell specification proceeds in an inseparably coordinated manner.[2] A transmembrane ligand, ephrinB2, and its receptor, the tyrosine kinase EphB4, are reported as molecular markers for arterial and venous endothelial cells (ECs), respectively.[3,4] Recently, various molecular markers specific for arterial ECs have been documented such as Delta-like 4 (Dll4), Bmx, Notch1, Activin receptor-like kinase 1 (Alk1), and others.[5,6] These findings enable the investigation of endothelial specification processes at the cellular and molecular levels being independent of the context of vessel location within the body plan.

The Notch pathway has been highlighted in arterial-venous specification.[7,8] Notch target genes, Hairy and Enhancer-of-split-related basic helix-loop-helix transcription factors, such as grl (gridlock) in zebrafish, or Hey1 and 2 in mammals, are required for arterial vascular development.[9,10] Arterial-venous specification mechanisms in zebrafish were further demonstrated to be a regulatory signaling cascade of sonic hedgehog-vascular endothelial growth factor (VEGF)-Notch-ephrinB2.[5] The molecular machinery for arterial-venous specification in mammals, however, is still undergoing investigation.

See page 1934

cAMP is a ubiquitous second messenger produced in cells and is involved in various biological phenomena including cell growth and differentiation.[11] Nevertheless, little has been reported for the role of cAMP signaling in vascular development. Adrenomedullin (AM) is a multifunctional polypeptide that was originally isolated from human pheochromocytoma.[12] AM exerts its function by increasing the levels of

Original received January 5, 2006; final version accepted May 17, 2006.

From the Laboratory of Stem Cell Differentiation (T.Y.-K., A.N., G.N., F.K., K.Y., M.H.-K., E.I., J.K.Y.), Stem Cell Research Center, Institute for Frontier Medical Sciences, Kyoto University, Japan; Department of Medicine and Clinical Science (T.Y.-K., H.I., K.N.), Kyoto University Graduate School of Medicine, Japan; Institute of Stem Cell Research (T.S.), GSF-National Research Center for Environment and Health, Germany; Department of Medical Systems Control (T.A., T.N.), Institute for Frontier Medical Sciences, Kyoto University, Japan; Institute of Biochemistry (U.J.), University of Kiel, Germany; Laboratory for Stem Cell Biology (S.-I.N.), Center for Developmental Biology, RIKEN, Japan; PRESTO (J.K.Y.), Japan Science and Technology Agency, Japan.

Correspondence to Jun K. Yamashita, Laboratory of Stem Cell Differentiation, Stem Cell Research Center, Institute for Frontier Medical Sciences, Kyoto University, 53 Shogoin Kawahara-cho, Sakyo-ku, Kyoto 606-8507 Japan. E-mail juny@frontier.kyoto-u.ac.jp

Arterioscler Thromb Vasc Biol. **is available at http://www.atvbaha.org** **DOI: 10.1161/01.ATV.0000234978.10658.41**

intracellular cAMP through the binding to its receptor complex, calcitonin receptor-like receptor (CRLR), and receptor activity modifying proteins (RAMP)-2 or RAMP-3.[13] Targeted null mutation of the AM gene shows embryonic lethality[14] with aberrant vascular formation and hemorrhage,[15] or extreme hydrops fetalis and cardiovascular abnormalities, including underdeveloped arterial walls,[16] inferring the significance of AM/cAMP signaling in vascular development.

Pluripotent embryonic stem (ES) cells are potent materials for both regenerative therapeutic approaches and developmental research. We have developed a novel ES cell differentiation system devoid of embryoid body formation or feeder cells that exhibits early vascular development using VEGF receptor-2 (VEGFR2)-positive cells as common progenitors for vascular cells.[17,18] We demonstrated that ES cell-derived VEGFR2$^+$ cells can differentiate into both ECs and mural cells (MCs) (pericytes and vascular smooth muscle cells) and form mature vascular-like structures in vitro.[18] Moreover, transplantation of induced vascular cells can augment the blood flow in tumor angiogenesis.[19] Our ES-derived VEGFR2$^+$ cell differentiation system can recapitulate the vascular development processes and dissect the cellular and molecular mechanisms of each developmental step including endothelial differentiation and specification.

In this study, we aimed to specifically induce arterial and venous ECs and elucidate the mechanisms of arterial-venous specification using our ES cell differentiation system. We successfully induced arterial and venous ECs and demonstrated that the AM/cAMP pathway is another indispensable signaling pathway in EC differentiation and arterial specification in conjunction with VEGF and Notch by reconstructing the arterial EC differentiation process in vitro. Our constructive approach using this ES cell system provides a novel understanding of the cellular and molecular mechanisms of vascular developmental processes.

Methods

Antibodies

Monoclonal antibodies for murine E-cadherin (ECCD2), murine VEGFR2 (AVAS12), and murine VE-cadherin (VECD1) were described previously.[18] Monoclonal antibodies for murine CD31 and CXCR4 were purchased from Pharmingen (San Diego, Calif). MoAb for murine alpha smooth muscle actin (SMA) 1A4 and human estrogen receptor-α (ERα) (F-10) antibody were from Sigma (St Louis, Mo) and Santa Cruz Biotechnology (Santa Cruz, Calif), respectively. Cleaved Notch1 antibody was from Cell Signaling Technology (Beverly, Mass).

Cell Culture

Induction of differentiation of an ES cell line, CCE (gift from Dr Evans), were performed using differentiation medium (alpha minimal essential medium; Gibco, Grand Island, NY) supplemented with 10% fetal calf serum (Equitech-Bio, Kerrville, Tex) and 5×10^{-5} mol/L 2-mercaptoethanol (Gibco) and VEGF165 (R&D System, Minneapolis, Minn) as previously described.[17,18] Other chemicals, rat AM (Peptide Institute, Inc, Osaka, Japan), 8-bromoadenosine-3′:5′-cyclic monophosphate sodium salt (8bromo-cAMP) (Nacalai Tesque, Kyoto, Japan), 8-bromoguanosine-3′:5′-cyclic monophosphate sodium salt (8bromo-cGMP) (Nacalai Tesque), 3-isobutyl-1-methyl-xanthine (IBMX) (Nacalai Tesque), or γ-secretase inhibitor IX, DAPT (Calbiochem, San Diego, Calif), and iloprost (Cayman Chemical, Ann Arbor, Mich) were occasionally added to VEGFR2$^+$ cell culture.

The recombination recognition sequence binding protein at the Jκ site (RBP-J$^{+/+}$), RBP-J$^{+/-}$ and RBP-J$^{-/-}$ D3 ES cell lines have been described previously.[20] The ES cell line NERT$^{\Delta O}$-7[21] was generated by stable introduction of CAG promoter-driven cDNA encoding a fusion protein of a constitutively active part of the intracellular domain of mouse Notch1 and a tamoxifen-sensitive mutant of the hormone binding domain of the human estrogen receptor α (NERT)[22] into EB5 ES cells (gift from Dr Niwa). To induce Notch activation, 4-hydroxytamoxifen (OHT) (50 to 500 nmol/L) (Sigma) was added to NERT$^{\Delta O}$-7 cell-derived VEGFR2$^+$ cells 12 hours after the plating. NERT$^{\Delta O}$-7/Hes-green fluorescent protein (GFP) cells were generated by stable introduction of Hes promoter-driven enhanced GFP (EGFP) gene[23] (gift from Dr Kageyama) into NERT$^{\Delta O}$-7 cells.

Flowcytometry and Cell Sorting

Fluorescence-activated cell sorting (FACS) of ES cells was performed as previously described.[17,18]

Immunocytochemistry

Immunostaining for cultured cells was performed as described.[18,24] Double immunofluorescent staining for CD31 and ERα was performed using anti-ERα antibody (1:50) and anti-CD31 antibody (1:300) as first antibodies, followed by second antibodies, Alexa Fluor 546-conjugated goat anti-rat IgG (1:500) and Alexa Fluor 488-conjugated goat anti-mouse IgG (1:500) (Molecular Probes, Eugene, Ore). For double staining for ephrinB2 and CD31, the fixed culture slides were incubated with EphB4-human immunoglobulin Fc portion chimeric protein (EphB4-Fc) (1:50; R&D system), followed by peroxidase-conjugated goat IgG fraction to human IgG Fc (1:500; ICN Biomedicals, Inc, Aurora, Ohio). TSA Biotin system (Tyramid signal amplification; PerkinElmer Life Science, Boston, Mass) was used for amplification of the signal for EphB4-Fc staining. EphrinB2$^+$ cells were visualized by using streptavidin-Alexa Fluor488-conjugate (Molecular Probes). Phycoerythrin-conjugated anti-CD31 antibody (Pharmingen) and DAPI (Molecular Probes) were added together with streptavidin-conjugated alexa 488. Cleaved intracellular domain of Notch (NICD) staining was performed using TSA Biotin System (PerkinElmer) with cleaved Notch1 antibody (1:300), followed by peroxidase-labeled anti-rabbit IgH (1:250; Vector Laboratories, Burlingame, Calif).

Single-Cell Analysis

Single-cell sorting of VEGFR2$^+$ cells using 96-well dishes was performed as previously described.[18] Colonies were stained for ephrinB2 using EphB4-Fc by TSA kit with streptavidin-conjugated horseradish peroxidase, followed by addition of phycoerythrin-conjugated anti-CD31 antibody and DAPI. Numbers of colonies including CD31$^-$ cells (EC-including), colonies including ephrinB2$^+$ cells (arterial EC-including), and ephrinB2$^+$ arterial EC numbers in each arterial EC-including colonies, as well as the total number of colonies that appeared were counted. 1692 VEGFR2$^+$ cells were cultured with VEGF alone, and 1128 cells were cultured with VEGF and 8bromo-cAMP. Total colony numbers in every 100 sequential wells, EC-including or arterial EC-including colony numbers in every 10 sequential colonies that appeared, and the arterial EC number in each arterial EC-including colony were statistically evaluated.

Measurement of Intracellular cAMP

After 3 days culture of VEGFR2$^-$ cells (2 to 10×10^5 cells), cells were harvested and counted. Intracellular cAMP concentration in total harvested cells was evaluated using cAMP Biotrak Enzyme Immunoassay system kit (Amersham Bioscience). Concentration was normalized by cell number.

In Situ Hybridization

In situ hybridization for CXCR4 was performed as previously described.[25]

Reverse-Transcription Polymerase Chain Reaction Amplification

Total RNA was isolated from sorted VE-cadherin$^+$ ECs induced by VEGF alone, or 8bromo-cAMP and VEGF treatment, using ISOGEN (Nippon Gene, Toyama, Japan). The reverse-transcription polymerase chain reaction was performed as described[25] using indicated primers (supplemental Table I, available online at http://atvb.ahajournals.org).

Statistical Analysis

Statistical analysis of the data was performed using Student t test. $P<0.05$ was considered significant.

Results

We first examined the effects of AM and cAMP on EC differentiation from ES cell-derived VEGFR2$^+$ progenitor cells. VEGFR2$^+$ cells were sorted by FACS and re-cultured for 3 days on type IV collagen-coated dishes in differentiation medium (see Methods) with VEGF (50 ng/mL) and other factors. Double immunostaining of induced cells with an EC marker, CD31, and a MC marker, SMA, revealed that VEGF treatment selectively induced both CD31$^+$ ECs and SMA$^+$ MCs from VEGFR2$^+$ cells as previously reported[15] (Figure 1A). Simultaneous stimulation of cAMP signaling in the presence of VEGF substantially enhanced EC induction from VEGFR2$^+$ cells (Figure 1B to 1D). VEGF together with 0.5 mmol/L 8bromo-cAMP resulted in substantial induction of ECs (Figure 1D), whereas 8bromo-cAMP treatment alone exerted almost no effect (data not shown). Another cyclic monophosphate analog, 8bromo-cGMP, showed no effect on VEGF-induced EC induction (data not shown). Addition of 10^{-6}mol/L AM also enhanced VEGF-stimulated EC induction, but to a lesser extent than 8bromo-cAMP (Figure 1B). Enhancement of the effect of AM by the simultaneous administration of a phosphodiesterase inhibitor, IBMX, revealed comparable EC induction with 8bromo-cAMP (Figure 1C). We quantitatively evaluated the EC-inducing effects of AM and 8bromo-cAMP using flow cytometry. VEGF treatment induced ECs to ≈30% of total cells. AM increased VEGF-induced ECs up to ≈50%. AM with IBMX or 8bromo-cAMP showed efficient induction of ECs to ≈70% of total cells (Figure 1E). Intracellular concentration of cAMP in the differentiating cells was significantly increased by AM with VEGF (667.6 fmol±215.1/10^6 cells; n=6; $P<0.01$ versus VEGF alone), or AM and IBMX with VEGF (1142 fmol±270.1/10^6 cells; n=6; $P<0.001$ versus VEGF alone) than that with VEGF alone (372.2 fmol±58.5/10^6 cells; n=6), and was comparable or lower level with those observed in previous reports using human umbilical vein ECs.[26] These results indicated that the AM/cAMP pathway specifically and synergistically enhances the effect of VEGF on EC differentiation from VEGFR2$^+$ progenitor cells.

Next, we investigated the features of induced ECs with AM/cAMP treatment with regard to arterial-venous diversity. Arterial ECs were evaluated by ephrinB2 expression, an arterial EC marker, detected by the binding of EphB4-Fc.[27]

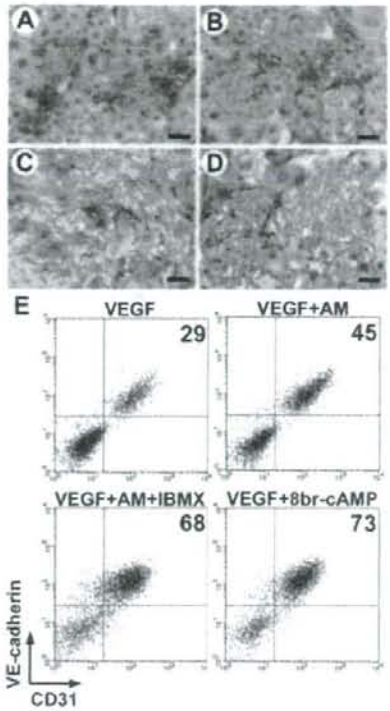

Figure 1. The effect of AM and cAMP on EC induction from VEGFR2$^+$ cells. A to D, Double immunostaining of induced ECs and MCs with an EC marker CD31 (purple) and MC marker SMA (brown) after 3 days of culture of VEGFR2$^+$ cells on type IV collagen-coated dishes in various conditions. A, VEGF treatment alone (50 ng/mL). CD31$^+$ EC sheets and SMA$^+$ MCs appear. B, VEGF with 10^{-6} mol/L AM. A slight increase of ECs is observed. C, VEGF with 10^{-6} mol/L AM and 10^{-4} mol/L IBMX. D, VEGF with 0.5 mmol/L 8bromo-cAMP. Remarkable EC induction occurs. Scale bars: 100 μm. E, Flow cytometry of induced cells from VEGFR2$^+$ cells with endothelial markers VE-cadhein and CD31. Left upper panel, VEGF treatment alone (50 ng/mL). Right upper panel, VEGF with 10^{-6} mol/L AM. Left lower panel, VEGF with 10^{-6} mol/L AM and 10^{-4} mol/L IBMX. Right lower panel, VEGF with 0.5 mmol/L 8bromo-cAMP. Percentages of VE-cadherin$^+$/CD31$^+$ ECs of total VEGFR2$^+$ cell-derived cells are indicated.

We double-immunostained ECs using anti-CD31 antibody and EphB4-Fc (Figure 2A to 2D). With VEGF treatment alone, very few ephrinB2$^+$ arterial ECs were observed among the ECs that appeared, indicating that venous ECs were mainly induced in this condition (Figure 2A). Surprisingly, remarkable appearance of ephrinB2$^+$ ECs was clearly observed by the stimulation of cAMP pathway. That is, addition of AM induced ephrinB2$^+$ EC appearance (Figure 2B). AM with IBMX, or 8bromo-cAMP together with VEGF, showed substantial induction of ephrinB2$^+$ ECs (Figure 2C and 2D). Messenger RNA expression of arterial EC markers, ephrinB2, Dll4, Notch1, Notch4, Alk1, and neuropilin1 (NRP1) were increased in 8bromo-cAMP and VEGF-treated ECs (Figure 2E). In contrast, venous EC markers, COUP-TFII transcription factor[28] and NRP2[29] mRNA were decreased by